ARMY RESEARCH LABORATORY

Design Considerations for the Diode-pumped Laser Ignition Project

by Jeffrey O. White

ARL-TN-0526 **January 2013**

NOTICES

Disclaimers

The findings in this report are not to be construed as an official Department of the Army position unless so designated by other authorized documents.

Citation of manufacturer's or trade names does not constitute an official endorsement or approval of the use thereof.

Destroy this report when it is no longer needed. Do not return it to the originator.

Army Research Laboratory
Adelphi, MD 20783-1197

ARL-TN-0526 **January 2013**

Design Considerations for the Diode-pumped Laser Ignition Project

Jeffrey O. White
Sensors and Electron Devices Directorate, ARL

REPORT DOCUMENTATION PAGE

Form Approved
OMB No. 0704-0188

1. REPORT DATE *(DD-MM-YYYY)*	2. REPORT TYPE	3. DATES COVERED (From - To)
January 2013	Final	June 2012 to August 2012

4. TITLE AND SUBTITLE
Design Considerations for the Diode-pumped Laser Ignition Project

5a. CONTRACT NUMBER

5b. GRANT NUMBER

5c. PROGRAM ELEMENT NUMBER

6. AUTHOR(S)
Jeffrey O. White

5d. PROJECT NUMBER

5e. TASK NUMBER

5f. WORK UNIT NUMBER

7. PERFORMING ORGANIZATION NAME(S) AND ADDRESS(ES)
U.S. Army Research Laboratory
ATTN: RDRL-SEE-M
2800 Powder Mill Road
Adelphi, MD 20783-1197

8. PERFORMING ORGANIZATION REPORT NUMBER
ARL-TN-0526

9. SPONSORING/MONITORING AGENCY NAME(S) AND ADDRESS(ES)

10. SPONSOR/MONITOR'S ACRONYM(S)

11. SPONSOR/MONITOR'S REPORT NUMBER(S)

12. DISTRIBUTION/AVAILABILITY STATEMENT
Approved for public release; distribution unlimited.

13. SUPPLEMENTARY NOTES

14. ABSTRACT
This technical note explores the design of the monolithic neodymium (Nd): yttrium aluminum garnet (YAG) laser used in the diode-pumped laser ignition system (DPLIS). Emphasis is placed on the divergence of the output beam and the dependence of the output power on misalignment of the mirrors polished on the two ends of the rod. A tradeoff between divergence and misalignment tolerance is identified and quantified. With input from the manufacturer on fabrication cost, the optimum design can be determined.

15. SUBJECT TERMS
Solid state laser, neodymium, diode pumping

16. SECURITY CLASSIFICATION OF:			17. LIMITATION OF ABSTRACT	18. NUMBER OF PAGES	19a. NAME OF RESPONSIBLE PERSON
a. REPORT	b. ABSTRACT	c. THIS PAGE			Jeffrey O. White
Unclassified	Unclassified	Unclassified	UU	24	19b. TELEPHONE NUMBER (*Include area code*) (301) 394-0069

Standard Form 298 (Rev. 8/98)
Prescribed by ANSI Std. Z39.18

Contents

List of Figures iv

List of Tables iv

Acknowledgments v

1. Introduction 1

2. Fundamental Mode Properties 1

3. Multimode Properties 4

4. Alignment Sensitivity 7

5. Discussion 9

6. Conclusion 10

7. References 11

Appendix. Matlab Program that Generated the Data 15

Distribution List 16

List of Figures

Figure 1. Geometry of the laser rod, cladding, and target. 1

Figure 2. TEM_{00} mode of the resonator, when $R1 = 5$ m, $L = 10$ cm, $R2 = \infty$. Spot size (top row) and radius of curvature (bottom) inside the laser (left column) and outside the laser (right). The target is located $T = 0.762$ m from M_2. 3

Figure 3. Contour plots of various quantities as a function of R_1 and L, for $R2 = \infty$: (upper left) ω_2, spot size of the fundamental mode at M_2; (upper right) M, i.e., the ratio of rod radius to spot size at M_2; (lower left) θ_m, divergence of multimode beam (half angle of cone that contains 87.5% of power); and (lower right) ω_T, spot size at target 0.762 m away from M_2. 6

Figure 4. Same quantities as in figure 3, plotted as a function of R_1 and R_2, for $L = 0.1$ m. 7

Figure 5. Contour plots of various quantities as a function of R_1 and L, for $R\mathbf{2} = \infty$: (top left) Mirror misalignment sensitivity D_1, (top right) D_2, (lower left) $1/D$, and (lower right) ωTD. 8

Figure 6. Contour plots of the same quantities as in figure 5, plotted as a function of R_1 and R_2, for $L = 0.1$ m. 9

List of Tables

Table 1. Spot sizes, divergences, and alignment sensitivity for specific values of L, R_1, and R_2. 4

Acknowledgments

This technical note follows from discussions with Mr. Gregory C. Burke at the U.S. Army Research Development and Engineering Command (*1*). He brought the problem to my attention and provided all the necessary background information. This technical note is an extension of analysis by Dr. Raymond L. Beach at Lawrence Livermore National Laboratory, described in a series of memoranda dated 9 April–2 August 2011 (*2*). Dr. Beach also furnished his Mathematica program, which was helpful in reconciling differences between his results and results obtained from my Matlab program.

INTENTIONALLY LEFT BLANK.

1. Introduction

This technical note explores the design of the monolithic neodymium (Nd): yttrium aluminum garnet (YAG) laser used in the diode-pumped laser ignition system (DPLIS). Emphasis is placed on the divergence of the output beam and the dependence of the output power on misalignment of the mirrors polished on the two ends of the rod. The design parameters include the radius of curvature of each mirror and the length of the rod. The DPLIS is a candidate to replace the primer-based ignition of propellant in a 155-mm howitzer. The DPLIS currently meets all the required specifications, but additional fluence would be desirable under conditions where the distance to the target is as large as 30 in (0.762 m) (*1*). Hence, the importance of minimizing the divergence.

2. Fundamental Mode Properties

The rod geometry and its relationship to the target are shown in figure 1. R_1 and R_2 are the radii of curvature of the two mirrors. L is the length of the rod and T is the distance to the target. Not counting the cladding surrounding the Nd-doped portion, the diameter of the rod is $2r$. A high reflectivity coating is applied to M_1 and a partially reflecting coating applied to M_2, the output coupler.

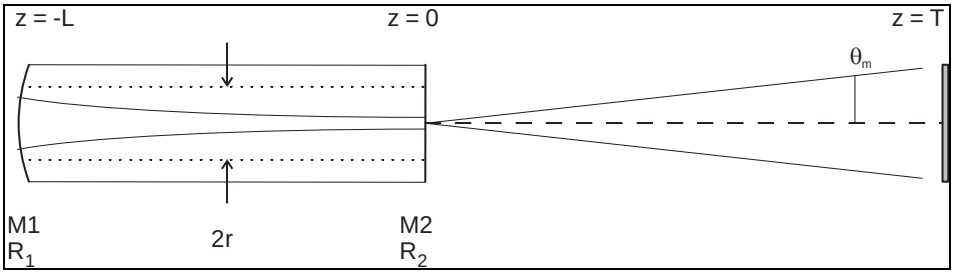

Figure 1. Geometry of the laser rod, cladding, and target.

We apply the usual analysis to determine the fundamental (TEM_{00}) mode inside and outside the cavity (*3*). The fundamental mode is defined if one knows the complex beam radius, q, at any point along the axis of propagation.

$$\frac{1}{q} = \frac{1}{\rho} - \frac{i\lambda}{\pi \mathrm{n} \omega^2} \tag{1}$$

where

λ is the wavelength. For the rest of this technical note, $\lambda = 1064$ nm.

ρ is the radius of curvature (r.o.c.) of the wavefront

n is the index of refraction of the medium. For YAG at 1064 nm, n = 1.82.

ω is the spot size. At a distance w from the axis, the intensity has decreased by $1/e^2$.

The complex beam radius incident upon M_2 is given by the solution of

$$q_2 = \frac{Aq_2 + B}{Cq_2 + D} \qquad \text{or} \qquad \frac{1}{q_2} = \frac{C + D/q_2}{A + B/q_2} \tag{2}$$

The latter form is convenient, given the relation of q to ρ and ω. When there's no lensing in the rod, the roundtrip matrix is given by

$$\begin{pmatrix} A & B \\ C & D \end{pmatrix} = \begin{pmatrix} 1 & L \\ 0 & 1 \end{pmatrix} \begin{pmatrix} 1 & 0 \\ -2/R_1 & 1 \end{pmatrix} \begin{pmatrix} 1 & L \\ 0 & 1 \end{pmatrix} \begin{pmatrix} 1 & 0 \\ -2/R_2 & 1 \end{pmatrix} \tag{3}$$

When $R_2 = \infty$, a waist forms at M_2 with a spot size ω_2 given by

$$\omega_2^2 = \omega_0^2 = \frac{\lambda}{\pi \, \mathrm{n}} \sqrt{L(R_1 - L)} \tag{4}$$

The radius of curvature of the beam matches that of the mirror at each end of the cavity. As an example, we calculate the fundamental mode for the case $R_1 = 5$ m, $L = 10$ cm, $R_2 = \infty$. The first column of figure 2 shows the spot size and radius of curvature inside the cavity. In the second column, the same quantities are shown between the laser and the target. The dashed lines indicate the asymptotic dependence. The Matlab© program that generated the data is reproduced in the appendix.

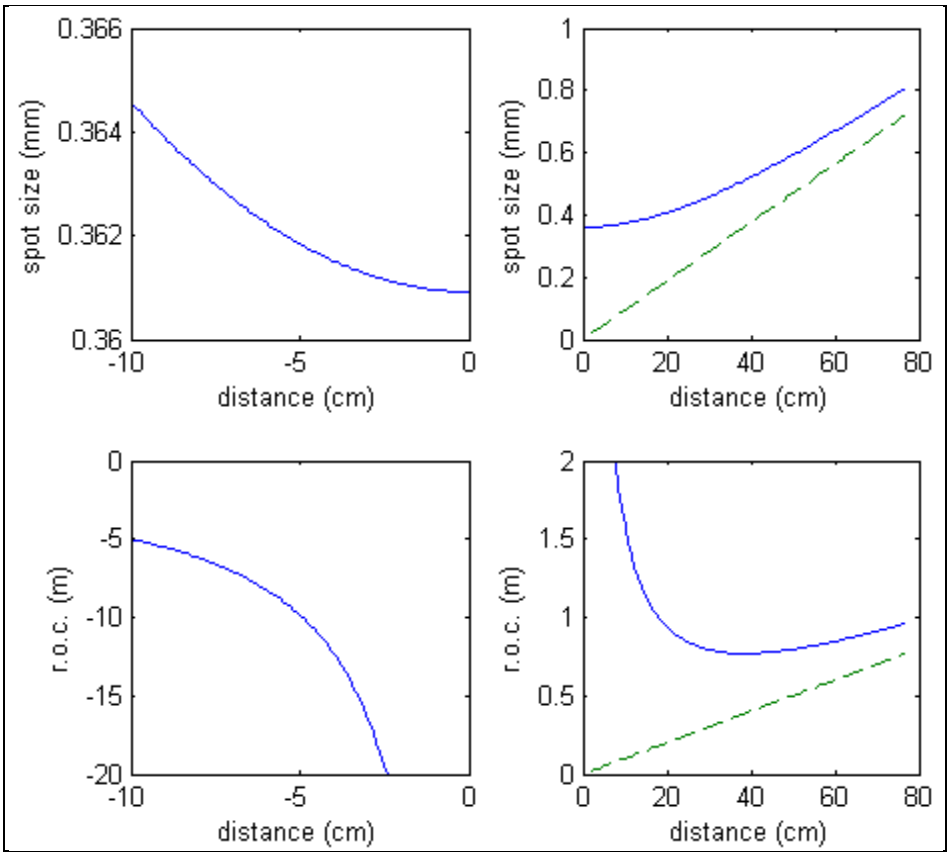

Figure 2. TEM_{00} mode of the resonator, when $R_1 = 5$ m, $L = 10$ cm, $R_2 = \infty$. Spot size (top row) and radius of curvature (bottom) inside the laser (left column) and outside the laser (right). The target is located $T = 0.762$ m from M_2.

Outside the cavity, in air, the divergence of the fundamental mode is given by

$$\theta_0 = \frac{\lambda}{\pi\omega_2} = \frac{\lambda \mathrm{n}}{\pi\sqrt{L(R_1 - L)}} \tag{5}$$

Table 1 shows ω_1, ω_2, and θ_0 for various choices of L and R_1, for the case $R_2 = \infty$. $R_1 > 10L$ in all cases. Two points can be made: (1) The spot sizes at the two mirrors are very close to one another, because the rod is short compared to R_1 and R_2 in all cases and (2) as R_1 increases, θ_0 decreases.

Table 1. Spot sizes, divergences, and alignment sensitivity for specific values of L, R_1, and R_2.

L (m)	R_1, HR (m)	R_2, OC (m)	ω_1 (mm)	ω_2 (mm)	θ_0 (mrad) half ∠	M	θ_m (mrad) half ∠	$\theta_m T$ (mm)	ω_T (mm)	D ($\times 10^4$)	($\omega_T D$) ($\times 10^3$)
0.1	1	∞	0.2491	0.2363	1.43	10.6	15.17	11.56	11.79	0.596	70.3
″	2	″	0.2922	0.2848	1.19	8.78	10.44	7.95	8.29	1.02	84.2
″	5	″	0.3646	0.3609	0.938	6.93	6.50	4.95	5.48	2.03	111
″	10	″	0.4325	0.4303	0.787	5.81	4.57	3.48	4.20	3.43	144
″	20	″	0.5136	0.5124	0.661	4.88	3.23	2.46	3.39	5.77	196
″	40	″	0.6104	0.6097	0.556	4.10	2.28	1.74	2.91	9.71	283
.075	1	″	0.2302	0.2214	1.53	11.3	17.27	13.16	13.37	0.645	86.2
″	2	″	0.2710	0.2649	1.27	9.40	11.97	9.12	9.42	1.09	103
″	5	″	0.3389	0.3363	1.01	7.43	7.49	5.70	6.17	2.19	135
″	10	″	0.4022	0.4007	0.845	6.24	5.27	4.02	4.65	3.69	171
″	20	″	0.4778	0.4770	0.710	5.24	3.72	2.84	3.68	6.20	228
″	40	″	0.5680	0.5675	0.597	4.41	2.63	2.00	3.08	10.4	322

3. Multimode Properties

For typical values of R_1 and R_2, a 5-mm-diameter rod ($r = 2.5$ mm) will lase with multiple transverse modes. The laser can be forced to lase in the fundamental mode, however, by introducing an aperture ~20% larger than the TEM_{00} spot size. Theoretically, one can also increase ω_1 and ω_2 to the point where the finite rod diameter suppresses the higher-order modes. However, this is impractical because it would require $R_1 \cong 5$ km.

The far-field divergence of a higher-order mode is given by

$$\theta_m = \sqrt{m + 1/2}\ \theta_0 \tag{6}$$

where m is the transversal order of the mode. According to reference 4, if an aperture is placed inside the resonator, and the rod is uniformly excited, the number of oscillating modes can be estimated by

$$m + 1/2 = (a/\omega_{0a})^2 \tag{7}$$

where

a is the radius of the aperture. For the remainder of this technical note, $a = r = 2.5$ mm.

ω_{0a} is the spot size of the fundamental mode at the position of the aperture.

In our case, rather than a conventional aperture at one fixed position, the Nd:YAG rod constitutes an aperture along the whole length of the rod, because the gain is zero everywhere outside the rod radius. However, the aperture is "soft" because the mirror diameter is equal to

that of the rod plus the cladding, so light travelling outside the rod can remain in the cavity, albeit with lower gain.

When $R_2 = \infty$, the multimode divergence is given by

$$\theta_m = \frac{\mathrm{n}r}{\sqrt{L(R_1 - L)}} = \frac{\lambda a}{\pi \omega_0^2} = \theta_0 \frac{a}{\omega_0} \tag{8}$$

The divergence has a minimum of $\theta_m = 1.82$ mrad for $R_1 = 2L$. This geometry is equivalent to half of a confocal resonator.

Note that if *m* modes are superimposed, with random phases, the beam would have a beam quality of $M^2 = m + 1/2$ in each transverse direction. The divergence and the spot size are each *M* times larger than the values for the fundamental mode; therefore, the net beam quality is M^2.

It is not clear why the divergence of the entire beam should be equal to that of the highest-order mode. Intuition would have it equal to some kind of average divergence of all the modes.

As a multimode beam propagates a distance T, the spot size increases approximately as (*5*)

$$\omega_\mathrm{T}^2 = \omega_{m2}^2 + (\theta_m T)^2 \tag{9}$$

where

ω_T is the radius of the spot that contains 87.5% of the power at the target, and

ω_{m2} is the multimode spot size at the beam waist, which is located at M_2 when $R_2 = \infty$. Because the multimode spot is not Gaussian, it is not obvious how to define the spot size, so we use the 87.5% criterion. The spot size of a TEM_{00} beam contains 87.5% of the power. For a uniform intensity profile inside the 2.5-mm-radius rod, a spot size of $\omega_{m2} = 2.34$ mm would contain 87.5% of the power.

θ_m is the multimode divergence.

T is the distance to the target.

Table 1 shows the calculated values for *M*, θ_m, $\theta_m T$, and ω_T for various choices of *L* and R_1, for the case $a = 2.5$ mm and $T = 0.762$ m. Four points can be made:

1. As R_2 increases, both *M* and θ_0 decrease, therefore θ_m decreases.
2. For the shorter values of R_1, ω_T is dominated by the divergence, i.e., $\omega_T \approx \theta_m T$.
3. For the larger values of R_1, e.g., $R_1 = 40$ m and $L = 0.1$ m, the divergence contributes only about 1/3 to the spot size; the rest is due to ω_{m2}.
4. The shorter rod length results in a larger ω_T.

The 6.5 mrad (half angle $1/e^2$) in row three agrees well with the 9-mrad divergence (full angle 50% power) measured experimentally*. Were the beam Gaussian, the latter would be equivalent to a 7.64-mrad half angle $1/e^2$ divergence.

The contour plots in figure 3 show ω_2 (for the fundamental mode), M, θ_m, and ω_T as a function of R_1 and L, for $R_2 = \infty$. The spot size at the target clearly decreases for larger values of R_1 and L. However, we expect the alignment sensitivity to increase as well.

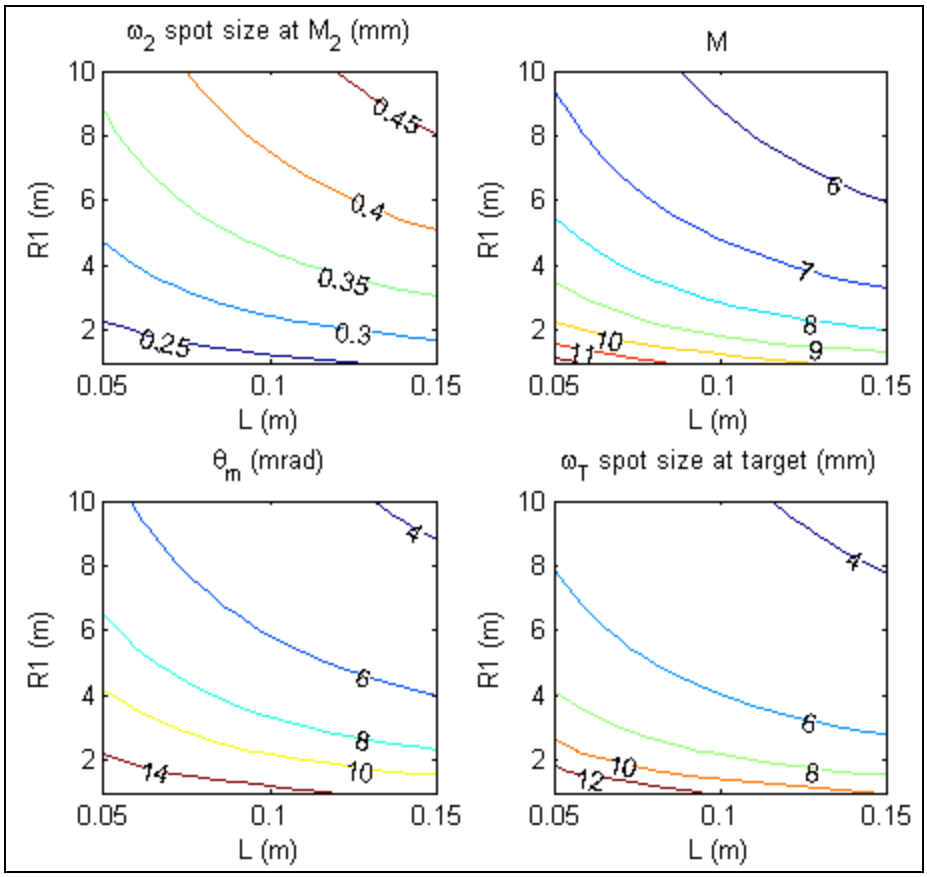

Figure 3. Contour plots of various quantities as a function of R_1 and L, for $R_2 = \infty$: (upper left) ω_2, spot size of the fundamental mode at M_2; (upper right) M, i.e., the ratio of rod radius to spot size at M_2; (lower left) θ_m, divergence of multimode beam (half angle of cone that contains 87.5% of power); and (lower right) ω_T, spot size at target 0.762 m away from M_2.

Next, we consider the impact of a finite positive radius of curvature on M_2. For the case $L = 0.1$ m, the spot sizes and divergence are shown in figure 4.

*The output coupler had a reflectivity of 50% (6).

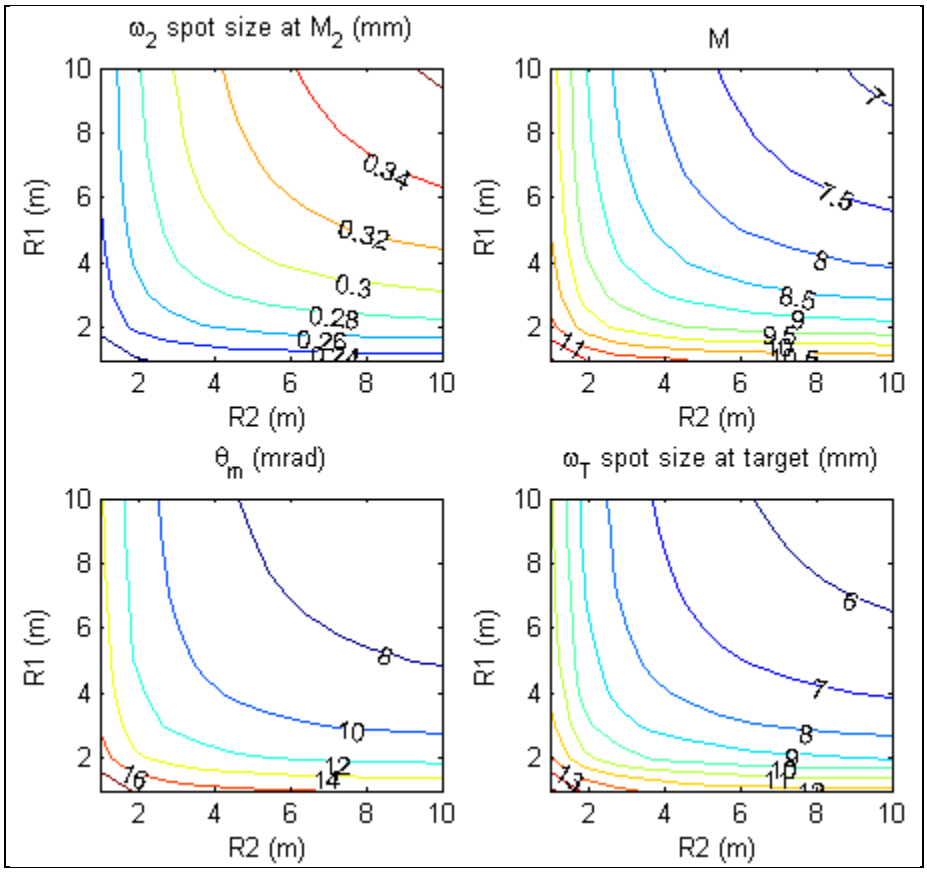

Figure 4. Same quantities as in figure 3, plotted as a function of R_1 and R_2, for $L = 0.1$ m.

4. Alignment Sensitivity

The alignment sensitivity for a *fundamental mode* two-mirror cavity with apertures at each mirror has been analyzed, and the analysis verified with experiment (*7*). Assuming small misalignments, i.e., small losses, and assuming that the apertures at each end of the rod are 1.2× the spot size, the misalignment sensitivity of M_i is given by

$$D_i^2 = \frac{\pi L}{\lambda}\sqrt{\frac{g_j}{g_i}}\cdot\frac{1+g_1g_2}{(1-g_1g_2)^{3/2}} \tag{10}$$

where $g_i = 1 - L/R_i$. If M_i is tilted by an angle of $1/D_i$, additional losses of ~10% are incurred (*4*). The combined sensitivity of the two-mirror cavity is defined as

$$D^2 = D_1^2 + D_2^2 \tag{11}$$

The alignment sensitivity would be at minimum for a confocal geometry (not shown in table 1). A disadvantage of the symmetric confocal geometry is the marginal stability in the ABCD matrix sense. Very small changes to R_1, R_2, or L can make the cavity unstable.

Equations 10 and 11 apply to a fundamental mode cavity. We make the assumption that they also apply to a multimode cavity if the aperture is equal to 1.2× the multimode spot size, which is approximately the case. The resulting values of D are shown in table 1. The trend should be meaningful even if the values are not quantitatively correct.

The top row of figure 5 are plots of D_1 and D_2 as a function of R_1 and L, for $R_2 = \infty$. It is clear that to reduce the sensitivity, one would want to decrease R_1. In the regime we are considering, L has less of an impact on D. The contour $D = 20{,}000$ corresponds to a misalignment of 50 µrad introducing a loss of 10%. Even though R_1 and R_2 are quite different, g_1 and g_2 are both close to one; therefore, D_1 is nearly the same as D_2. Figure 5c shows the misalignment angle that would introduce an additional loss of 10%, based on the combined sensitivity.

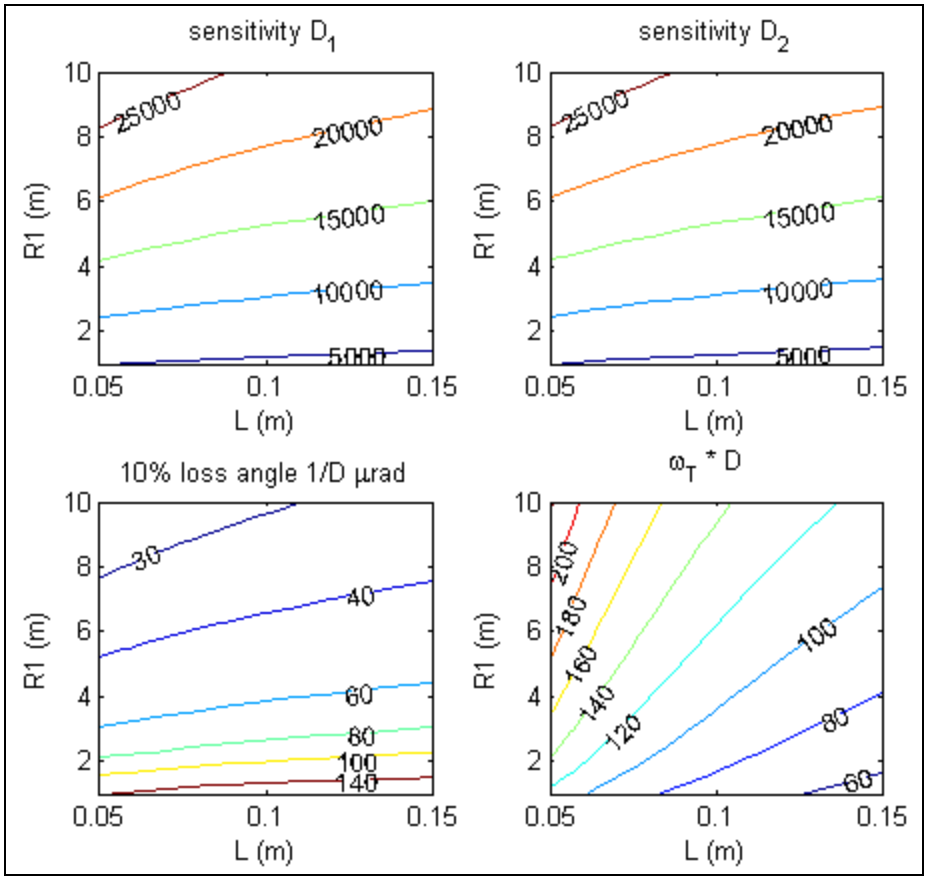

Figure 5. Contour plots of various quantities as a function of R_1 and L, for $R_2 = \infty$: (top left) Mirror misalignment sensitivity D_1, (top right) D_2, (lower left) $1/D$, and (lower right) $\omega_T D$.

We take the product $\omega_T D$ to be a figure of *de*merit, i.e., the larger the product the less desirable the cavity. The values of $\omega_T D$ for specific values of R_1 are shown in table 1. The product is shown in figure 5 (lower left) as a function of R_1 and L. The contour labeled 100 corresponds, for example, to a divergence of 1 mrad and an alignment tolerance of 10 μrad.

The same quantities are plotted in figure 6, as a function of R_1 and R_2, for the case $L = 0.1$ m.

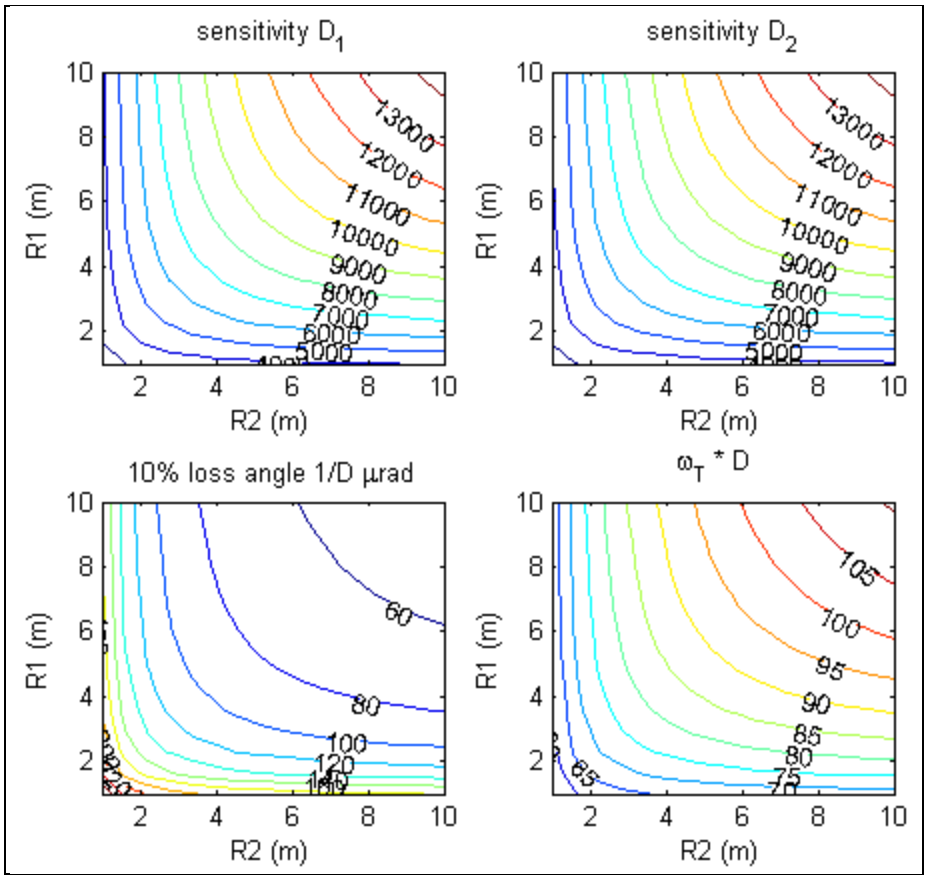

Figure 6. Contour plots of the same quantities as in figure 5, plotted as a function of R_1 and R_2, for $L = 0.1$ m.

5. Discussion

The three design parameters that can easily be adjusted are L, R_1, and R_2. According to the above results, a longer L is desirable; however, L is limited to 10 cm by the space available in the breech. It is also clear from the preceding analysis that larger mirror radii of curvature yield a smaller spot on the target, and thus higher fluence for a given pulse energy. However, a choice of optimum R_1 and R_2 has to be informed by the difficulty (or cost) in meeting the required parallelism tolerance, which increases with R. Another avenue to pursue is an optimization of the output coupler reflectivity. Adding a lens next to the pressure window might also be helpful.

Making the window into a positive lens by curving one surface is also being explored (*1*).

6. Conclusion

The analysis presented in this report quantifies the known tradeoffs associated with varying the radius of curvature of the mirrors polished on the rod in the DPLIS. Increases in radius of curvature decrease the divergence of the output beam, which is good, but they also make more stringent the parallelism of the two mirrors, which adds to the cost of fabrication.

7. References

1. Burke, G.C. Private communication, 2012 U.S. Army ARDEC; RDAR-WSW-I, Picatinny Arsenal, NJ 07806-5000, gregory.burke2@us.army.mil.
2. Beach, R. L. Private communication, 2012 Lawrence Livermore National Laboratory, Livermore, CA 94551. beach2@llnl.gov.
3. Yariv, A. *Quantum Electronics*; 2nd ed.; John Wiley & Sons, 1975.
4. Kortz, H. P.; Iffländer, R.; Weber, H. Stability and Beam Divergence of Multimode Lasers with Internal Variable Lenses. *Appl. Opt.* **1981**, *20*, 4124–4134.
5. Silfvast, W. T. Laser Fundamentals, 2nd ed. (Cambridge University Press, 2004) pg. 423.
6. Burke, G.C. "Laser gain media divergence study test report," unpublished, 2011.
7. Hauck, R.; Kortz, H. P.; Weber, H. Misalignment Sensitivity of Optical Resonators. *Appl. Opt.* **1980**, *19*, 598–601.

INTENTIONALLY LEFT BLANK.

Appendix. Matlab Program that Generated the Data

The following is the Matlab program that generated the data.

```
function [zv,wv,rhov,w2,theta0,M,D1,D2,spotT] = wrho(R1,L,R2,T,printfig)
% outputs z,w,rho,theta0,M,D,spot size at target given R1,L,R2,T
% when printfig is set to 1, a figure is displayed showing the results
global wl n r
fprintf('R1= %6.2e m\n',R1);     %
fprintf('L = %6.2e m\n',L);     %
fprintf('R2= %6.2e m\n',R2);     %
fprintf('T = %6.2e m\n',T);     %

M2 = [1 L; 0 1] * [1 0;-2/R1 1] * [1 L; 0 1] * [1 0; -2/R2 1];    % at M2
A2 = M2(1,1);   B2 = M2(1,2);   C2 = M2(2,1);   D2 = M2(2,2);
fprintf('A= %6.2e B= %6.2e C= %6.2e D=%6.2e\n\n',A2,B2,C2,D2);

ooq2i = ((D2-A2)-sqrt((D2-A2)^2+4*B2*C2))/(2 * B2);
fprintf('1/q2i = %6.2e %6.2e mm\n',real(ooq2i),imag(ooq2i) );          %
% ooq2i = (D2-A2)/(2 * B2) - 1i * sqrt(1- ( (D2+A2)/2)^2) / B2; % from Kortz
% fprintf('1/q2i = %6.2e %6.2e mm\n',real(ooq2i),imag(ooq2i) );          %

q2i = 1/ooq2i;
fprintf('q2i = %6.2e %6.2e mm\n',real(q2i),imag(q2i) );          %
w2i = w_qn(q2i,n);
w2  = w2i;

q2e = q2i / ( (1-n)/R2*q2i + n );       %propagate through OC into air
rho2e = rho_q(q2e);
w2e = w_qn(q2e,1);                       % index of 1
theta0 = atan(wl / (pi*w2e) );
M = r / w2e;                    % how many time diff ltd
thetam = theta0 * M;
g1 = 1-L/R1;
g2 = 1-L/R2;
prefactor = (pi*L/wl)*(1+g1*g2)/(1-g1*g2)^1.5;
D1s = prefactor*sqrt(g2/g1);
D2s = prefactor*sqrt(g1/g2);
D1  = sqrt(D1s);
D2  = sqrt(D2s);
D   = sqrt(D1s+D2s);
Da  = D;
Ds = prefactor*abs(g1+g2)/sqrt(g1*g2);
Db = sqrt(Ds);

spotTs = 0.875*r^2 + (thetam * T)^2;
spotT = sqrt(spotTs);

ziv   = linspace(-L,0,100);
qiv   = q2i + ziv;
wiv   = w_qn(qiv,n);
rhoiv = rho_q(qiv);
```

```
zev   = linspace(0,T,100);
qev   = q2e + zev;
wev   = w_qn(qev,1);
rhoev = rho_q(qev);
wav   = zev * wl / pi / w2e;              % waist asymptotic

zv   = cat(2,ziv,zev);
wv   = cat(2,wiv,wev);
rhov = cat(2,rhoiv,rhoev);

fprintf('spot at M1 = %10.3e mm\n',wiv(1)*1000);          %
fprintf('roc  at M1 = %6.2e m\n',rhoiv(1));       %
fprintf('spot at M2 = %10.3e mm\n',w2i*1000);          %
fprintf('roc  at M2 = %6.2e m\n',rho2e);        %
fprintf('theta0     = %6.3f mrad\n',theta0*1000);      %
fprintf('M= %6.2e\n',M);          %
fprintf('thetam   = %6.2f\n',thetam*1000);          %
fprintf('thetam  T= %6.2f mm\n',thetam*T*1000);          %
fprintf('spot at T= %6.2f mm\n\n',spotT*1000);          %
fprintf('D1     = %6.2e \n',D1);
fprintf('D2     = %6.2e \n',D2);
fprintf('Da     = %6.2e \n',Da);
% fprintf('Db     = %6.2e \n',Db);
% fprintf('thetam D = %6.2e \n',thetam*Da);
fprintf('spotT * D = %6.2e \n',spotT*Da);
% fprintf('1/(spotT D)= %6.2e \n\n',1/(spotT*Da));

if printfig==1;
    figure8x10(1);
    subplot(3,2,1,'Visible','off');
    annotation('textbox',...
               'Position',get(gca,'Position'),'String',...
                {'wrho.m';...
                ['R1= ' num2str(R1) 'm L= '  num2str(L)] ;...
                ['R2= ' num2str(R2) '  T= '  num2str(T)] ;...
                ['spotsize @HR= ' num2str(wiv(  1)*1000,'%5.3f') 'mm'] ;...
                ['         @OC= ' num2str(wev(  1)*1000,'%5.3f')] ;...
                ['    @target= ' num2str(wev(end)*1000,'%5.3f')] ;...
                ['D1 = ' num2str(D1,'%6.2e') ];...
                ['D2 = ' num2str(D2,'%6.2e') ];...
                ['D  = ' num2str(D ,'%6.2e') ];...
                });

    subplot(3,2,2,'Visible','off');
    annotation('textbox',...
               'Position',get(gca,'Position'),...
               'String',{datestr(now);...
                         ['n= '  num2str(n)];...
                         ['\lambda= ' num2str(wl*1e6) ' um'];...
                         ['r= ' num2str(r) ' mm'];...
                         ['\theta0= ' num2str(theta0*1000,'%5.3f') '
mrad'];...
                         ['M= ' num2str(M)];...
                         ['\thetam = ' num2str(thetam*1000,'%6.2f')];...
                         ['\thetam D ' num2str(thetam * D,'%6.2e')]});
```

```
    subplot(3,2,3);
    plot(ziv*100,wiv*1000);
    xlabel('distance (cm)');
    ylabel('spot size (mm)');
    % v = axis;
    % axis([ v(1) v(2) 0.36 0.365])

    subplot(3,2,4);
    plot(zev*100,wev*1000,'-'); %,zev*100,wav*1000,'--');
    xlabel('distance (cm)');
    ylabel('spot size (mm)');

    subplot(3,2,5);
    plot(ziv*100,max(-4*R1,min(4*R1,rhoiv)) );
    xlabel('distance (cm)');
    ylabel('r.o.c. (m)');
%     v = axis;
%     axis([ v(1) v(2) v(3) 0])

    subplot(3,2,6);
    plot(zev*100,max(-5*T,min(5*T,rhoev)),'-'); %,zev*100,zev,'--') ;
    xlabel('distance (cm)');
    ylabel('r.o.c. (m)');
%     v = axis;
%     axis([ v(1) v(2) 0 R2]);
end

function w = w_qn(qv,n)
% calculate spot size given q vector and index of refraction
global wl
w = sqrt( -wl ./ (pi * n * imag(1./qv) ) );

function rho = rho_q(qv)
% calculate radius of curvature given q vector
rho = 1./ (real(1./qv));

global wl n r
wl = 1.064e-6;    % m
n = 1.82;         %  Nd:YAG at 1.06
r = 2.5e-3;       % rod radius (m)
```

1 (PDF only) DEFENSE TECHNICAL INFORMATION CTR
DTIC OCA
8725 JOHN J KINGMAN RD
STE 0944
FORT BELVOIR VA 22060-6218

1 HC DIRECTOR
US ARMY RESEARCH LAB
IMAL HRA
2800 POWDER MILL RD
ADELPHI MD 20783-1197

1 HC DIRECTOR
US ARMY RESEARCH LAB
RDRL CIO LL
2800 POWDER MILL RD
ADELPHI MD 20783-1197

5 HC JEFFREY O WHITE
RDRL-SEE-M
2800 POWDER MILL RD
ADELPHI MD 20783-1197

5 HC GREGORY C BURKE
US ARMY ARDEC
RDAR WSW I
BLDG 61
PICATINNY ARSENAL, NJ 07806-5000

1 HC GARY L WOOD
RDRL SEE
2800 POWDER MILL RD
ADELPHI, MD 20783-1197

1 HC LAWRENCE M. STOUT
RDRL SEE M
2800 POWDER MILL RD
ADELPHI, MD 20783-1197